

Original Research Paper

Altered brain network function during attention-modulated visual processing in multiple sclerosis

Dániel Veréb , Eszter Tóth, Bence Bozsik, András Király, Nikoletta Szabó, Bálint Kincses, Krisztián Kocsis, Péter Faragó, Vécsei László, Krisztina Bencsik, Péter Klivényi and Zsigmond Tamás Kincses 

Abstract

Background: Multiple sclerosis may damage cognitive performance in several domains, including attention. Although attention network deficits were described during rest, studies that investigate their function during task performance are scarce.

Objective: To investigate connectivity within and between task-related networks in multiple sclerosis during a visual attention task as a function of cognitive performance.

Methods: A total of 23 relapsing-remitting multiple sclerosis (RRMS) patients and 29 healthy controls underwent task-functional magnetic resonance imaging (fMRI) scans using a visual attention paradigm on a 3T scanner. Scans were analysed using tensor-independent component analysis (TICA). Functional connectivity was calculated within and between components. We assessed cognitive function with the Brief International Cognitive Assessment for MS (BICAMS) battery.

Results: TICA extracted components related to visual processing, attention, executive function and the default-mode network. Subject scores of visual/attention-related and executive components were greater in healthy controls ($p < 0.032$, $p < 0.023$). Connectivity between visual/attention-related and default-mode components was higher in patients ($p < 0.043$), correlating with Brief Visuospatial Memory Test–Revised (BVMT-R) scores ($R = -0.48$, $p < 0.036$). Patients showed reduced connectivity between the right intraparietal sulcus (rIPS) and frontal eye field (rFEF), and bilateral frontal eye fields ($p < 0.012$, $p < 0.003$). Reduced rIPS-rFEF connectivity came with lower Symbol Digit Modalities Test (SDMT)/BVMT-R scores in patients ($R = 0.53$, $p < 0.02$, $R = 0.46$, $p < 0.049$).

Conclusion: Attention-related networks show altered connectivity during task performance in RRMS patients, scaling with cognitive disability.

Keywords: Relapsing-remitting multiple sclerosis, cognitive disability, visuospatial attention, functional MRI, model-free analysis

Date received: 9 February 2020; revised: 28 June 2020; accepted: 18 August 2020.

Introduction

Changes of connectivity in large-scale networks were previously described in relapsing-remitting multiple sclerosis (RRMS) in resting state and during tasks (multiple sclerosis (MS); see, for example, Tahedl et al.¹ for a review). Resting state and task-related networks share a common architecture that is utilised during task performance;² therefore, altered resting-state connectivity might give rise to dysfunctional network activity in response to a task. The hallmark pathological alterations of the

white matter in MS, namely macroscopic lesions and diffuse microstructural damage, cause disruption in neuronal networks that may underlie the aforementioned changes.³ These changes might also affect the communication between networks, causing global functional reorganisation.⁴ The breakdown in network structure and disrupted inter-network communication might explain the usual pattern of neuropsychological dysfunction in MS patients,⁵ which involves cognitive functions evoked by the coordinated interaction of many

Multiple Sclerosis Journal

1–9

DOI: 10.1177/
1352458520958360© The Author(s), 2020.
Article reuse guidelines:
sagepub.com/journals-
permissions

Correspondence to:

ZT Kincses
Neuroimaging Research
Group, Department of
Radiology, Albert Szent-
Györgyi Clinical Center,
University of Szeged,
Semmelweis u. 6, 6725
Szeged, Hungary.
kincses.zsigmond.tamas@
med.u-szeged.hu

Dániel Veréb
Eszter Tóth
Bence Bozsik
András Király
Nikoletta Szabó
Bálint Kincses
Krisztián Kocsis
Péter Faragó
Vécsei László
Krisztina Bencsik
Péter Klivényi
Department of Neurology,
Albert Szent-Györgyi
Clinical Center, University of
Szeged, Szeged, Hungary
Zsigmond Tamás Kincses
Department of Neurology,
Albert Szent-Györgyi
Clinical Center, University
of Szeged, Szeged, Hungary/
Neuroimaging Research
Group, Department of
Radiology, Albert Szent-
Györgyi Clinical Center,
University of Szeged,
Szeged, Hungary

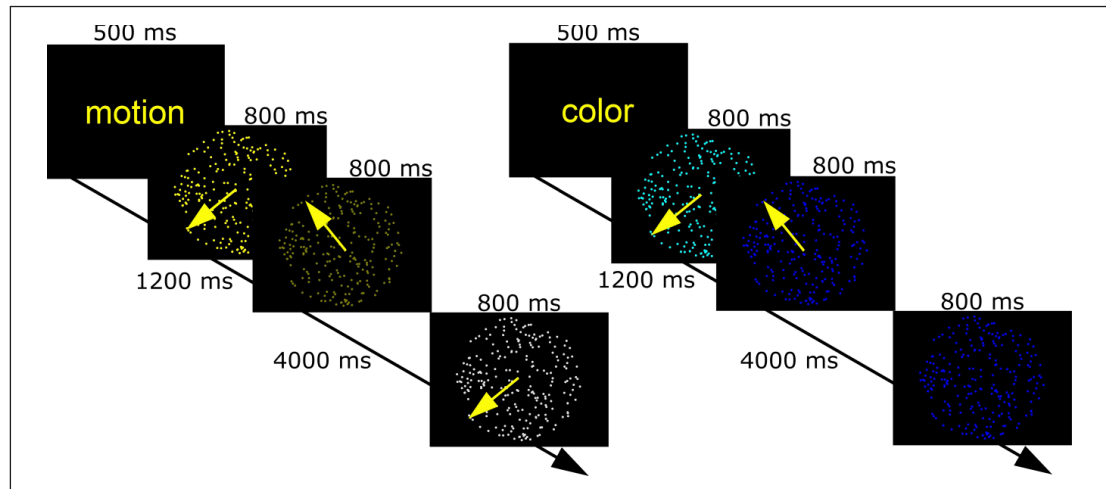


Figure 1. Task protocol. The figure depicts one trial of the motion and colour conditions used in the random dot kinematogram task. Each trial was followed by an 8.1-second response period, where participants had to decide whether the main attribute of the target stimulus (direction of motion or shade of colour) appeared among the two previous stimuli.

different brain regions, such as executive functions, memory and attention.⁶

Attention regulates sensory processes in both a tonic and phasic manner,⁷ with the former usually involving top-down mechanisms and the latter guided by stimulus-driven changes in attention. Both systems are possibly affected in MS.⁸ So far, studies mostly focused on characterising brain networks underlying attention during rest in MS, showing that these networks exhibit altered intrinsic connectivity in patients that is associated with clinical and cognitive disability.⁹ However, task-based investigation of attention-related brain activity in MS patients has mostly been confined to activation studies.¹⁰ Although these studies established a pattern of altered activity in attention-related brain regions, they did not investigate how these regions interact during a task.

Our aim was to characterise connectivity differences within and between attention-related networks during a visual attention task between healthy participants and RRMS patients.

Materials and methods

Task design

We employed a modified random dot kinematogram paradigm, in which participants watch a circular aperture containing coherently moving dots (kinematograms).¹¹ In this case, the dots coherently move in a random direction and are of a single colour. At the start

of each trial, a text message appeared for 0.5 seconds, warning participants to pay attention to a specific attribute of consequent stimuli (shade of colour or direction of motion). Afterwards, two consecutive random dot kinematograms were displayed for 0.8 seconds each, with a 1.2-second interstimulus interval. The second stimulus was followed by a target stimulus displayed for 0.8 seconds after a rest period of 4 seconds. Participants had 8.1 seconds before the next trial to decide whether the relevant attribute of the target was the same as it had been in one of the previous two kinematograms. Each trial lasted for 16.2 seconds (including the time given to respond), and there were 20 trials for each condition (40 altogether). For a depiction of the task, see Figure 1.

Participants

A total of 23 patients with RRMS and 29 healthy controls participated in this study. All patients are treated at the Multiple Sclerosis Outpatient Clinic, at the Department of Neurology, University of Szeged and were diagnosed according to the revised McDonald criteria¹² by neurologists with >10 years of experience. Patients were in stable clinical condition, meaning they did not relapse 6 months prior to the scans and afterwards. All patients received disease-modifying treatment (3 interferon β -1 α , 5 glatiramer acetate, 1 natalizumab, 2 alemtuzumab, 3 dimethyl fumarate, 5 teriflunomide, 4 fingolimod). Healthy participants did not suffer from any neuropsychiatric illnesses, and patients did not have additional neuropsychiatric conditions apart from RRMS. All participants had

Table 1. Demographic and clinical data of the participants.

Group	MS	HC
<i>N</i>	23	29
Age in years	39.01 (± 8.83)	40.76 (± 13.03)
Sex (female/male)		
Motion during the scan (FD)	0.0024 \pm 0.0006	0.0023 \pm 0.0007
EDSS	1.31 (± 1.49 , 0–5)	–
Disease duration	9.35 (± 6.69)	–
Number of T2-hyperintense lesions (median and range)	17 (4–73)	–
Lesion volume (cm ³ , median and range)	25.03 (0.58–47.04)	–

FD: framewise displacement; EDSS: Expanded Disability Status Scale; MS: multiple sclerosis; HC: healthy control.

normal or corrected-to-normal vision and reported no difficulty performing the task. Demographic and clinical data are included in Table 1. According to the Helsinki Declaration, we acquired written consent from all participants, and the local ethics committee approved the study (reference no. 35/2017).

Cognitive testing

We assessed cognitive function in the MS group using the electronic version of the validated Hungarian Brief International Cognitive Assessment for MS (BICAMS) test battery.¹³ This battery has been developed to quickly assess cognitive functions often affected in MS and includes three tests: the Symbol Digit Modalities Test (SDMT) that measures the speed of information processing; the Brief Visuospatial Memory Test–Revised (BVMT-R) which measures visuospatial short-term memory; and the immediate recall part of the California Verbal Learning Test 2 which measures verbal short-term memory.¹⁴

Image acquisition

Three-dimensional (3D) T1-weighted fast spoiled gradient echo images (FSPGR-IR, TR: 5.3 ms TE: 2.1 TI: 450 ms, slice thickness: 1 mm, matrix: 512 \times 512, FOV: 256 mm \times 256 mm, slice no. 312, whole-brain coverage, flip angle: 12°) and T2*-weighted BOLD EPI images (TR: 2500 ms, TE: 27 ms, 44 mm \times 3 mm axial slices providing whole-brain coverage, FOV: 288 mm \times 288 mm; matrix: 96 \times 96, flip-angle: 81°, interleaved acquisition scheme) were acquired on a 3T GE MR750W Discovery scanner (GE, Milwaukee, USA). The functional magnetic resonance imaging (fMRI) protocol comprised the acquisition of 270 volumes, which took approximately 12 minutes. Stimuli were displayed on a screen in the scanner room via a video projector. Participants saw the screen through a mirror applied to the head coil frame. We did not

match stimuli onset times to volume acquisition times in order to allow for sub-second temporal resolution in the time series analysis.

Preprocessing

Preprocessing steps were performed via FEAT 6.0 as contained in the FMRIB Software Library (FSL, v5.0.10).¹⁵ The first five volumes were discarded to avoid saturation effects. Motion correction was applied using a rigid body (6 DOF) registration to the middle volume with MCFLIRT. We additionally quantified subject motion by calculating the framewise displacement (FD) for each subject.¹⁶ There were no differences in motion parameters between groups (mean FD between groups: independent-samples *T*-test, $p > 0.05$). Following slice-timing correction and grand-mean intensity scaling, non-brain tissue was removed from the images. Resulting volumes were normalised to the individual T1-weighted images using boundary-based registration, then further transformed to standard 2 mm MNI-space using nonlinear registration as implemented in FSL FNIRT. For the multivariate analysis, volumes were resampled into 4 mm standard space. Prior to registration, lesion filling was performed on the T1-weighted images using the lesion_filling tool included in FSL to improve registration accuracy.¹⁷

Statistical analysis

Group-level independent component analysis. We performed a multivariate analysis of the activation maps using the tensorial extension of independent component analysis (TICA) as implemented in FSL MELODIC.¹⁸ TICA is an exploratory analysis method that does not rely on pre-defined time-series models. During a complex task, cognitive performance is supported by large-scale distributed networks, and studies show that even background

activity is often modulated by task demands.¹⁹ Therefore, the underlying structure of the data in this case is less predictable beforehand, which renders traditional hypothesis-based methods (like the general linear model (GLM) approach) less effective. TICA performs a simultaneous tri-linear decomposition of all participants' data into independent component matrices, which describe spatial, temporal and subject-dependent dimensions. This tri-linear combination is optimised via a least-squares approach so that different modes are maximally independent or non-Gaussian. MELODIC thresholds spatial maps via an alternative hypothesis test based on fitting a Gaussian/Gamma mixture model to the distribution of voxel intensities within spatial maps and a posterior probability threshold of $p > 0.5$. Data dimensionality was estimated automatically using the Laplace approximation to the Bayesian evidence of the model order, which divided the data into 29 independent components (ICs). We classified ICs as signal or noise based on resemblance to known functional networks in spatial and temporal properties (this was done by visual inspection following recent guidelines),²⁰ adherence to the task timeline (quantified by the a posteriori GLM-based analysis of network time series) and consistence across subjects (meaning the absence of outliers in the overall pool of individual subject modes). To determine the relationship between network expression and clinical parameters, Spearman's rank correlation was calculated between IC subject modes and disease duration, Expanded Disability Status Scale (EDSS) scores, lesion number and volume and total number of relapses in the MS group. We assessed the potential association between network expression and cognitive functions by calculating the partial Spearman's rank correlation (controlling for age, sex, years spent in education and disease duration) between subject modes and the scores of all three BICAMS subtests (SDMT, BVMT-R, California Verbal Learning Test–second edition (CVLT-II)) in the MS group.

To assess voxel wise activation differences between the two groups, an additional univariate analysis was carried out in IC2 and IC6, with the same first-level design as in the post hoc regression analysis, using FSL FEAT. The statistical analysis of voxel wise time series was performed using FILM with local autocorrelation correction.²¹ We carried out the higher-level analysis of group differences with FLAME, which is contained in FEAT 6.0.²² Z (Gaussianised T) statistic images were pre-masked using the probability masks of IC2 and IC6 estimated by TICA, then thresholded using clusters determined by $Z > 3.1$ and a corrected cluster significance threshold of $p = 0.05$.²³

Within-network functional connectivity. To assess functional connectivity within networks extracted by the group ICA, component probability maps were thresholded at $p = 0.9$ and binarised, then masked using the 100-parcel version of the cortical atlas by Schaefer et al.²⁴ Time series were extracted from the masked probability maps by taking the mean of all voxels underlying a given parcel. We chose this atlas because parcels are matched to the 7-network parcellation by Yeo et al.²⁵

Between-network functional connectivity. In order to determine individual time series underlying each IC, we used a dual regression approach to recover subject-specific component maps.²⁶ These were thresholded at 99% (to minimise the connectivity bias introduced by cross-subject differences in the spatial configuration of and overlap between networks),²⁷ binarised and used to extract subject-specific network time series, defined as the mean time series of all underlying voxels.

Time series analysis. We analysed time series data using the FSLNets toolbox (<https://fsl.fmrib.ox.ac.uk/fsl/fslwiki/FSLNets>). Within-network functional connectivity was calculated separately for each IC in each participant as the partial Pearson's correlation between regional time series. This metric describes direct connectivity between two time series over and above connectivity to other time series; therefore, it provides information about residual stimulus-related oscillations over and above the main task effect.²⁸ Between-network functional connectivity was calculated as the pairwise Pearson's correlation of all selected ICs. The estimated correlation matrices were fed into a group-level GLM and evaluated by a non-parametric permutation test to assess group differences of within- and between-network connectivity. Results were corrected for multiple comparisons by controlling the family-wise error rate. To assess whether and how within/between-component connectivity and BICAMS subscores are related in the MS group, we calculated the partial Pearson's correlation, controlling for age, sex, education and disease duration.

Results

Group ICA

We selected ICs 1, 2, 4 and 6 as valid components. IC1 comprised the bilateral extrastriate cortices (V2-4), and regions considered part of the top-down attention system: frontal eye fields (FEF), medial frontal regions, intraparietal sulci and anterior caudate nuclei.

IC2 contained the bilateral lower-level visual cortices, bilateral intraparietal sulci and bilateral FEFs. IC4 consisted of areas that resemble the default-mode network (ventromedial prefrontal cortex, precuneus, bilateral angular gyri and superior temporal gyri). IC6 comprised the anterior cingulate cortex, the ventral frontal cortex and superior parietal lobule on the right and the bilateral insulae and striate cortices, representing a conjunct activation of the ventral attention system, salience network and motor cortex. The spatial maps of ICs are depicted in Figure 2.

A post hoc regression analysis was carried out on the estimated component time courses, using an event-related design that coded the onset of the cue, the colour and motion conditions, and contained the target as nuisance regressor to exclude effects of task performance. IC1 and IC2 showed greater activation in the motion condition ($p < 0.001$ and $p < 0.049$). IC4, the default-mode network anticorrelated with the task design as expected.

Subject modes of IC2 and IC6 showed significant differences between healthy controls and patients, with lower scores in the MS group ($p < 0.032$ and $p < 0.023$, respectively).

In IC2, a significant cluster showing greater activation during the motion condition in the healthy group was detected in the right premotor cortex ($p < 0.044$).

Correlation with clinical parameters and cognitive function

We found no correlation between clinical parameters or cognitive performance and the expression of IC2 and IC6. However, higher expression of IC1 and IC4 came with significantly lower SDMT scores, controlled for age, sex, education years and disease duration ($R = -0.50$, $p < 0.029$ and $R = -0.49$, $p < 0.032$, respectively). BVMT-R and CVLT-II scores did not show any significant association to subject modes.

Within-network functional connectivity

Figure 3 shows the mean pattern of partial correlation in IC2 nodes. Partial correlation was lower between the right anterior intraparietal sulcus and the right frontal eye field, as well as between the bilateral frontal eye fields in the MS group in IC2 ($p < 0.012$ and $p < 0.003$, corrected for multiple comparisons). A stronger connection between the right intraparietal sulcus and right frontal eye field came with higher SDMT and BVMT-R scores, controlled

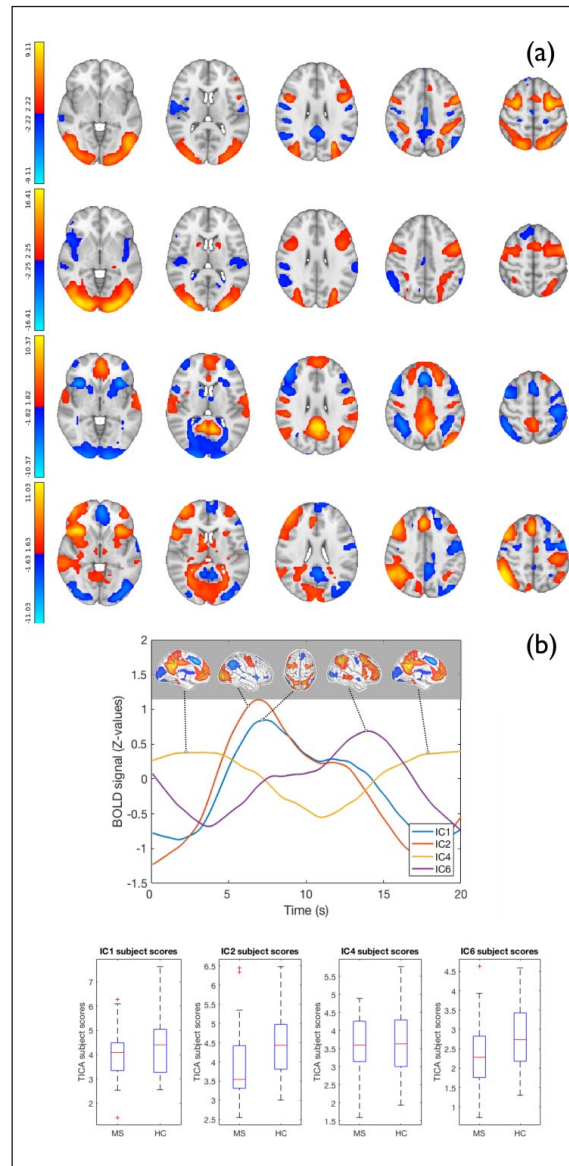


Figure 2. Results of the tensor-independent component analysis. (a) Spatial maps of IC1, 2, 4 and 6. Probability maps of each IC were thresholded at $p = 0.9$, registered to 1 mm spatial resolution and overlaid on a standard MNI152 template. The colour bar shows Z-values. Deactivations (depicted in blue-light blue) represent networks anticorrelated with the current IC. For details, see the corresponding section. (b) Average timeline of network activations during a single trial. To establish a timeline of network dynamics after the stimuli appear, we created a post-stimulus plot from each network's time courses by pooling data points that were sampled from each trial in a window that comprised 20 seconds starting from the appearance of the first stimulus. As our TR was not matched to stimulus timings, we were able to estimate a millisecond resolution plot of network activations in the post-stimulus time window. Boxplots show subject scores of each IC in the two groups as estimated by the TICA analysis.

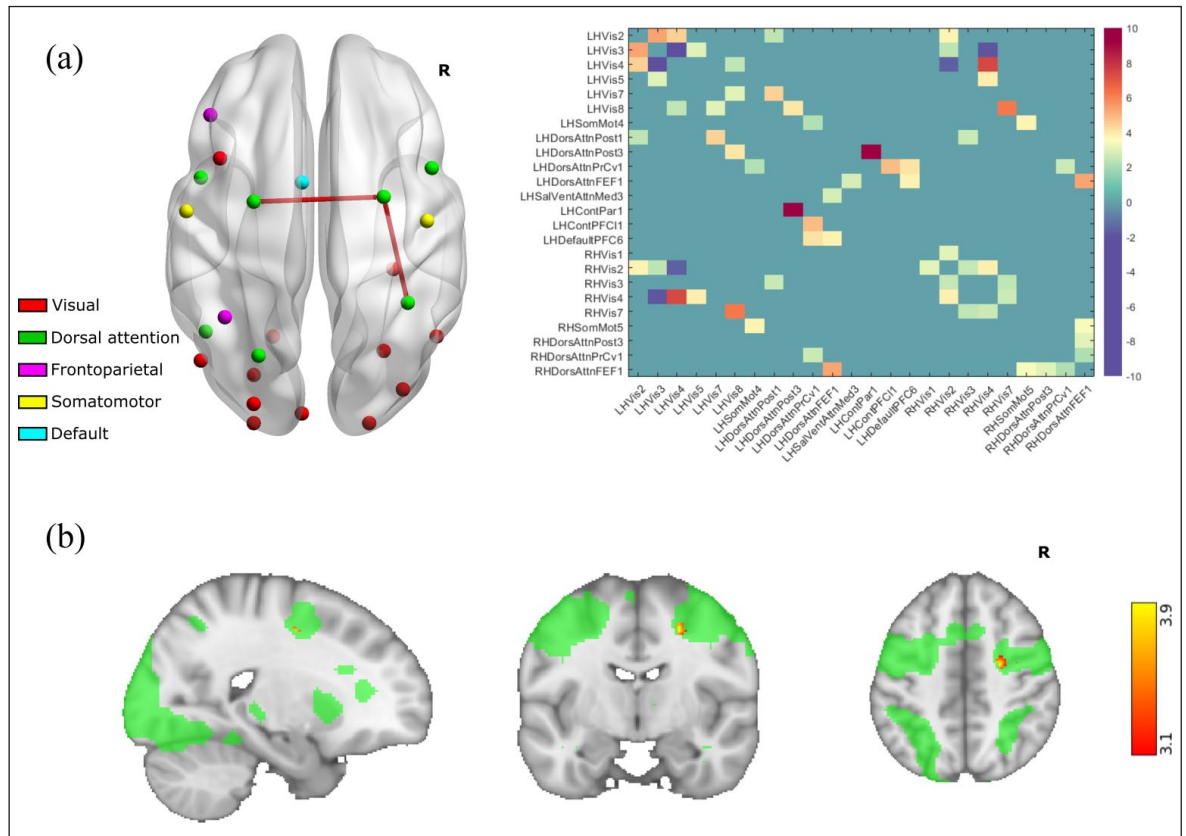


Figure 3. Regional connectivity and activation differences in IC2. (a) Nodes of IC2 were overlaid on the smoothed ICBM52 template. The figure shows edges that differ significantly between the healthy and MS groups. The correlation matrix depicts the average Z-transformed partial correlation between nodes in the healthy group, containing edge weights that were consistently strong according to a t -statistic ($t > 6$). Node labels are taken from the Schaefer atlas. (b) Results of the univariate analysis, depicting the right frontal eye field with significantly smaller activation during the motion condition in multiple sclerosis patients within IC2. The binarised component map used for pre-threshold masking is shown in green. The thresholded Z-statistic was upsampled to 1 mm resolution and overlaid on the MNI152 template (cluster maximum MNI coordinates: $x=26, y=-2, z=48$). The colour bar depicts Z-values.

for age, sex, education and disease duration in the MS group ($R=0.53, p < 0.02$ and $R=0.46, p < 0.049$). No group differences were observed in IC6 connectivity.

Between-network functional connectivity

IC1 and IC2 were positively correlated on average in both groups (healthy control (HC): $R_{1-2}=0.68$, MS: $R_{1-2}=0.67$), and both of them were uncorrelated with IC6 (HC: $R_{1-6}=0.13$ and $R_{2-6}=0.01$, MS: $R_{1-6}=0.03$ and $R_{2-6}=-0.18$). IC4, the default mode network showed negative correlation on average to all other ICs in both groups (HC: $R_{1-4}=-0.37, R_{2-4}=-0.24$ and $R_{6-4}=-0.5$, MS: $R_{1-4}=-0.3, R_{2-4}=-0.08$ and $R_{6-4}=-0.54$). Differences between network couplings were found in the case of IC2-IC4, which showed stronger correlation (a lesser extent of anticorrelation) in the MS group ($p < 0.043$).

Discussion

In this study, we showed that the expression of certain task-specific networks is altered in RRMS patients while performing a visual attention task. One of these components (IC2) depicted visual information encoding together with activation of fronto-parietal regions. The spatial features of this network resemble the dorsal attention and visual networks. The temporal resolution of our experiment did not allow for separating the tonic attentional control and the activation of the visual system because of the duration of the cue stimulus and the slowness of the hemodynamic response. A second component (IC6) was also altered, in which the salience network, ventral attentional network and motor activity were integrated.

The voxel wise analysis of task-related activation in IC2 revealed decreased activation in the right frontal eye field, which is consistent with a meta-analysis of

attention-related activation differences between healthy controls and MS patients showing decreased activation in similar locations.¹⁰ Decreased activation in this location might have contributed to the altered expression of IC2 in MS patients.

IC2 also showed decreased within-network and increased between-network connectivity according to our results. Specifically, connectivity between IC2 and IC4, the default-mode network was altered in the MS group, exhibiting diminished anticorrelation. The anticorrelated activity of task-positive and task-negative networks is thought to support cognitive function.^{29,30} Although previous studies reported that both the default mode and dorsal attention networks show altered connectivity patterns as a function of cognitive performance in MS,^{9,31} the connectivity between these networks has been less frequently investigated. A study described preserved anticorrelation structure between the default-mode and dorsal attention network during rest, with increased interaction between the two networks.³² Our results suggest that this anticorrelation structure might be perturbed during task performance. Additionally, IC2-IC4 connectivity correlated with BVMT-R scores in the MS group, which is in line with previous studies linking the anticorrelated activity of task-positive and task-negative networks to working memory performance.³⁰

Interestingly, we found decreased connectivity between the right anterior intraparietal sulcus and frontal eye field in IC2 throughout the task. These regions are the backbone of the dorsal attention network,⁷ and the right frontal eye field also showed reduced activation during the motion condition according to our results. Although studies previously described alterations in the functional connectivity of attention networks during rest,^{9,33} our results show that these connections remain dysfunctional in the face of task demands as well.

Our result that higher correlation between attention-related areas is connected to better SDMT performance complements previous descriptions of attention deficits in MS being related to processing speed.⁸ These connections also scale with BVMT-R performance, which might stem from shared resources between visuospatial attention and working memory.³⁴ Processing speed also plays a part in BVMT-R performance.³⁵

There are some methodological limitations to consider in this study. As our temporal resolution is in the seconds domain, sequentially activating

networks do not differ enough in their time course for TICA to differentiate them as separate components. Additionally, we did not explicitly test for colour sight in the patient group, though patients reported no difficulty performing the task. Finally, here we use a complex cognitive task involving multiple cognitive domains, and further studies are required to investigate the neural correlates of specific aspects of the attention system in MS.

Our results correspond to the growing body of research that shows reorganisation of brain networks in multiple sclerosis during rest and task performance.³⁶ Functional adaptation of networks has implications in the prognosis of MS, as plastic changes seem to be closely related to the patients' cognitive performance.³⁷ Also, network plasticity is being increasingly exploited for its therapeutic value in cognitive rehabilitation.³⁸ Seeing as maladaptive changes in brain function appear early, future work should aim to establish a timeline of functional changes during the disease course, which could help develop improved rehabilitation strategies that take dysfunctional network adaptation into account.

Conclusion

In this study, we found altered connectivity within and between task-related networks during a visual attention task in RRMS patients that correlates with cognitive disability.

Acknowledgements

We thank MRI operators János Laczi and Zoltán Tóth for their invaluable help with the measurements.


Declaration of Conflicting Interest

The author(s) declared no potential conflicts of interest with respect to the research, authorship and/or publication of this article.

Funding

The author(s) disclosed receipt of the following financial support for the research, authorship and/or publication of this article: The study was supported by the Neuroscience Research Group of the Hungarian Academy of Sciences and the University of Szeged, GINOP-2.3.2-15-2016-00034 grant, EFOP-3.6.1-16-2016-00008, by a Horizon 2020 grant (H2020-MSCA-RISE-2016 734718), NAP 2.0 (2017-1.2.1-NKP-2017-00002), National Brain Research Program (KTIA_13_NAP-A-II/20) and the Bolyai Scholarship Programme of the Hungarian Academy of Sciences.

ORCID iDs

Dániel Veréb  <https://orcid.org/0000-0003-2077-5252>

Zsigmond Tamás Kincses  <https://orcid.org/0000-0002-1442-4475>

References

1. Tahedl M, Levine SM, Greenlee MW, et al. Functional connectivity in multiple sclerosis: Recent findings and future directions. *Front Neurol* 2018; 9: 828.
2. Smith SM, Fox PT, Miller KL, et al. Correspondence of the brain's functional architecture during activation and rest. *Proc Natl Acad Sci United Stat Am* 2009; 106: 13040–13045.
3. Zhou F, Zhuang Y, Gong H, et al. Altered inter-subregion connectivity of the default mode network in relapsing remitting multiple sclerosis: A functional and structural connectivity study. *PLoS ONE* 2014; 9(7): e101198.
4. Sbardella E, Tona F, Petsas N, et al. Functional connectivity changes and their relationship with clinical disability and white matter integrity in patients with relapsing-remitting multiple sclerosis. *Mult Scler* 2015; 21(13): 1681–1692.
5. Di Filippo M, Portaccio E, Mancini A, et al. Multiple sclerosis and cognition: Synaptic failure and network dysfunction. *Nat Rev Neurosci* 2018; 19(10): 599–609.
6. Langdon DW. Cognition in multiple sclerosis. *Current Opinion Neurol* 2011; 24: 244–249.
7. Corbetta M and Shulman GL. Control of goal-directed and stimulus-driven attention in the brain. *Nat Rev Neurosci* 2002; 3(3): 201–215.
8. Vázquez-Marrufo M, Galvao-Carmona A, González-Rosa JJ, et al. Neural correlates of alerting and orienting impairment in multiple sclerosis patients. *PLoS ONE* 2014; 9(5): e97226.
9. Rocca MA, Valsasina P, Leavitt VM, et al. Functional network connectivity abnormalities in multiple sclerosis: Correlations with disability and cognitive impairment. *Mult Scler* 2018; 24(4): 459–471.
10. Kollndorfer K, Krajnik J, Woitek R, et al. Altered likelihood of brain activation in attention and working memory networks in patients with multiple sclerosis: An ALE meta-analysis. *Neurosci Biobehav Rev* 2013; 37(10 Pt. 2): 2699–2708.
11. Zanto TP and Gazzaley A. Neural suppression of irrelevant information underlies optimal working memory performance. *J Neurosci* 2009; 29: 3059–3066.
12. Polman CH, Reingold SC, Banwell B, et al. Diagnostic criteria for multiple sclerosis: 2010 revisions to the McDonald criteria. *Ann Neurol* 2011; 69(2): 292–302.
13. Sandi D, Rudisch T, Fuvesi J, et al. The Hungarian validation of the brief international cognitive assessment for multiple sclerosis (BICAMS) battery and the correlation of cognitive impairment with fatigue and quality of life. *Mult Scler Relat Disord* 2015; 4(6): 499–504.
14. Langdon DW, Amato MP, Boringa J, et al. Recommendations for a brief international cognitive assessment for multiple sclerosis (BICAMS). *Mult Scler* 2012; 18(6): 891–898.
15. Smith SM, Jenkinson M, Woolrich MW, et al. Advances in functional and structural MR image analysis and implementation as FSL. *Neuroimage* 2004; 23(Suppl. 1): S208–S219.
16. Jenkinson M, Bannister P, Brady M, et al. Improved optimization for the robust and accurate linear registration and motion correction of brain images. *Neuroimage* 2002; 17(2): 825–841.
17. Battaglini M, Jenkinson M and De Stefano N. Evaluating and reducing the impact of white matter lesions on brain volume measurements. *Hum Brain Mapp* 2012; 33(9): 2062–2071.
18. Beckmann CF and Smith SM. Tensorial extensions of independent component analysis for multisubject fMRI analysis. *Neuroimage* 2005; 25(1): 294–311.
19. Tamas Kincses Z, Johansen-Berg H, Tomassini V, et al. Model-free characterization of brain functional networks for motor sequence learning using fMRI. *Neuroimage* 2008; 39: 1950–1958.
20. Griffanti L, Douaud G, Bijsterbosch J, et al. Hand classification of fMRI ICA noise components. *Neuroimage* 2017; 154: 188–205.
21. Woolrich MW, Ripley BD, Brady M, et al. Temporal autocorrelation in univariate linear modeling of FMRI data. *Neuroimage* 2001; 14(6): 1370–1386.
22. Woolrich MW, Behrens TE, Beckmann CF, et al. Multilevel linear modelling for FMRI group analysis using Bayesian inference. *Neuroimage* 2004; 21(4): 1732–1747.
23. Worsley KJ, Liao CH, Aston J, et al. A general statistical analysis for fMRI data. *Neuroimage* 2002; 15(1): 1–15.
24. Schaefer A, Kong R, Gordon EM, et al. Local-global parcellation of the human cerebral cortex from intrinsic functional connectivity MRI. *Cerebral Cortex* 2018; 28: 3095–3114.
25. Yeo BT, Krienen FM, Sepulcre J, et al. The organization of the human cerebral cortex estimated

- by intrinsic functional connectivity. *J Neurophysiol* 2011; 106(3): 1125–1165.
26. Nickerson LD, Smith SM, Ongur D, et al. Using dual regression to investigate network shape and amplitude in functional connectivity analyses. *Front Neurosci* 2017; 11: 115.
 27. Bijsterbosch JD, Woolrich MW, Glasser MF, et al. The relationship between spatial configuration and functional connectivity of brain regions. *Elife* 2018; 7: e32992.
 28. Spisak T, Pozsgay Z, Aranyi C, et al. Central sensitization-related changes of effective and functional connectivity in the rat inflammatory trigeminal pain model. *Neuroscience* 2017; 344: 133–147.
 29. Santarnecchi E, Emmendorfer A, Tadayon S, et al. Network connectivity correlates of variability in fluid intelligence performance. *Intelligence* 2017; 65: 35–47.
 30. Hampson M, Driesen N, Roth JK, et al. Functional connectivity between task-positive and task-negative brain areas and its relation to working memory performance. *Magn Reson Imag* 2010; 28(8): 1051–1057.
 31. van Geest Q, Douw L, van 't Klooster S, et al. Information processing speed in multiple sclerosis: Relevance of default mode network dynamics. *Neuroimage Clin* 2018; 19: 507–515.
 32. Huang M, Zhou F, Wu L, et al. Synchronization within, and interactions between, the default mode and dorsal attention networks in relapsing-remitting multiple sclerosis. *Neuropsychiatr Dis Treat* 2018; 14: 1241–1252.
 33. Louapre C, Perlberg V, Garcia-Lorenzo D, et al. Brain networks disconnection in early multiple sclerosis cognitive deficits: An anatomofunctional study. *Hum Brain Mapp* 2014; 35(9): 4706–4717.
 34. Feng J, Pratt J and Spence I. Attention and visuospatial working memory share the same processing resources. *Front Psychol* 2012; 3: 103.
 35. Tam JW and Schmitter-Edgecombe M. The role of processing speed in the brief visuospatial memory test: Revised. *Clin Neuropsychol* 2013; 27(6): 962–972.
 36. Pantano P, Mainero C and Caramia F. Functional brain reorganization in multiple sclerosis: Evidence from fMRI studies. *J Neuroimaging* 2006; 16(2): 104–114.
 37. Helekar SA, Shin JC, Mattson BJ, et al. Functional brain network changes associated with maintenance of cognitive function in multiple sclerosis. *Front Hum Neurosci* 2010; 4: 219.
 38. Tomassini V, Matthews PM, Thompson AJ, et al. Neuroplasticity and functional recovery in multiple sclerosis. *Nature Rev Neurol* 2012; 8: 635–646.

Visit SAGE journals online
[journals.sagepub.com/
 home/msj](http://journals.sagepub.com/home/msj)

 SAGE journals